Author Manuscript

Author Manuscript

Author Manuscript

Author Manuscript

HHS Public Access

Author manuscript

*Toxicology*. Author manuscript; available in PMC 2020 November 01.

Published in final edited form as:

*Toxicology*. 2019 November 01; 427: 152283. doi:10.1016/j.tox.2019.152283.

# The trichloroethylene metabolite *S*-(1,2-dichlorovinyl)-L-cysteine induces progressive mitochondrial dysfunction in HTR-8/SVneo trophoblasts

**Elana R. Elkin**[a], **Dave Bridges**[b], **Rita Loch-Caruso**[a]

[a]Department of Environmental Health Sciences, University of Michigan, 1415 Washington Heights, Ann Arbor, MI 48109-2029 USA

[b]Department of Nutritional Sciences, University of Michigan, 1415 Washington Heights, Ann Arbor, MI 48109-2029 USA

## Abstract

Trichloroethylene is an industrial solvent and common environmental pollutant. Despite efforts to ban trichloroethylene, its availability and usage persist globally, constituting a hazard to human health. Recent studies reported associations between maternal trichloroethylene exposure and increased risk for low birth weight. Despite these associations, the toxicological mechanism underlying trichloroethylene adverse effects on pregnancy remains largely unknown. The trichloroethylene metabolite *S*-(1,2-dichlorovinyl)-L-cysteine (DCVC) induces mitochondrial-mediated apoptosis in a trophoblast cell line. To gain further understanding of mitochondrial-mediated DCVC placental toxicity, this study investigated the effects of DCVC exposure on mitochondrial function using non-cytolethal concentrations in placental cells. Human trophoblasts, HTR-8/SVneo, were exposed *in vitro* to a maximum of 20 μM DCVC for up to 12 h. Cell-based oxygen consumption and extracellular acidification assays were used to evaluate key aspects of mitochondrial function. Following 6 h of exposure to 20 μM DCVC, elevated oxygen consumption, mitochondrial proton leak and sustained energy coupling deficiency were observed. Similarly, 12 h of exposure to 20 μM DCVC decreased mitochondrial-dependent basal, ATP-linked and maximum oxygen consumption rates. Using the fluorochrome TMRE, dissipation of mitochondrial membrane potential was detected after a 12-h exposure to 20 μM DCVC and (±)-α-tocopherol, a known suppressor of lipid peroxidation, attenuated DCVC-stimulated mitochondrial membrane depolarization but failed to rescue oxygen consumption perturbations. Together, these results suggest that DCVC caused progressive mitochondrial dysfunction, resulting in lipid peroxidation-associated mitochondrial membrane depolarization. Our findings contribute to the

Corresponding Author Rita Loch-Caruso, PhD, Department of Environmental Health Sciences, University of Michigan, 1415 Washington Heights, Ann Arbor, MI, USA, 48109-2029, rlc@umich.edu.

Supplementary Material

Supplementary material is available.

**Publisher's Disclaimer:** This is a PDF file of an unedited manuscript that has been accepted for publication. As a service to our customers we are providing this early version of the manuscript. The manuscript will undergo copyediting, typesetting, and review of the resulting proof before it is published in its final form. Please note that during the production process errors may be discovered which could affect the content, and all legal disclaimers that apply to the journal pertain.

Conflict of Interest

The authors declare that there are no conflicts of interest.

Author Manuscript Author Manuscript Author Manuscript Author Manuscript

biological plausibility of DCVC-induced placental impairment and provide new insights into the role of the mitochondria in DCVC-induced toxicity.

**Keywords**

Trichloroethylene (TCE); *S*-(1,2-dichlorovinyl)-L-cysteine (DCVC); mitochondria; placenta; extravillous trophoblasts

## 1. Introduction

Trichloroethylene (TCE) is a volatile organic compound used for decades as a dry-cleaning solvent and industrial metal degreaser. Due to longstanding use and improper disposal, persistent TCE environmental contamination continues to pose a potential hazard to human health. TCE has proven to be a potent organ-and organ system-specific toxicant (Lash et al. 2014; Waters et al. 1977). For example, TCE is classified by the National Toxicology Program (NTP) and International Agency for Research on Cancer as a known human carcinogen based on epidemiological evidence and animal toxicity studies demonstrating that the compound causes kidney cancer in humans and animals (Guha et al. 2012; Lash et al. 2000b; NTP 2015; Rusyn et al. 2014). Moreover, TCE has been implicated in adverse pregnancy outcomes. Although an early study found no association (Lagakos et al. 1986), several recent studies described significant associations between maternal TCE exposure and increased risk of low birth weight (Forand et al. 2012; Ruckart et al. 2014). Despite these reports, many aspects of the TCE toxicological mechanism of action remain unknown.

Optimal placental function is critical for a healthy pregnancy. Abnormal placental development may play a key role in adverse birth outcomes (Ilekis et al. 2016). For example, placental insufficiency originating from deficient placental structure and/or function may contribute to preterm birth risk (Morgan 2014; Morgan 2016). Indeed, pre-eclampsia, which involves placental abnormalities, is associated with increased risk of preterm birth and low birth weight (Davies et al. 2016; Oshvandi et al. 2018)

Furthermore, as a highly perfused organ with abundant metabolic activity, the placenta is a probable target organ for toxicity (Goodman et al. 1982). Because the placenta has a large surface area that serves as the maternal-fetal interface, it is readily exposed to any TCE and TCE metabolites circulating in maternal blood (Burton and Fowden 2015; Laham 1970). Moreover, the placenta (Lee et al. 2013; Myllynen et al. 2005; Nishimura and Naito 2006), as well as placenta-derived cell lines (Hassan et al. 2016; Wu et al. 2019), express many enzymes required for TCE metabolism including cytochrome P450, glutathione-S-transferase and cysteine conjugate beta-lyase. The presence of these enzymes greatly increases the risk of placenta-generated toxic TCE metabolites.

Specific TCE metabolites are implicated in TCE toxicity, suggesting that TCE metabolism is required to exert its toxic effects (Lash et al. 2014; Lash et al. 2000a). Previous studies in models without metabolic capabilities have shown little to no TCE-induced genotoxicity (Cichocki et al. 2016). On the other hand, many studies have described cytotoxicity to specific TCE metabolites. Notably, multiple *in vitro* studies have demonstrated that the

Author Manuscript Author Manuscript Author Manuscript Author Manuscript

glutathione pathway-derived metabolite *S*-(1, 2-dichlorovinyl)-L-cysteine (DCVC) is toxic to kidney proximal tubular cells, following further transformation by the enzyme beta-lyase, to several unstable reactive thiol species (Chen et al. 1990; Lash et al. 2000a) in rodents and humans (Chen et al. 2001; Darnerud et al. 1989; Lash and Anders 1986; Lash et al. 2001; Xu et al. 2008). Furthermore, mechanistic studies revealed that DCVC cytotoxicity in kidney cells is mediated by mitochondrial dysfunction, aberrant reactive oxygen species (ROS) generation, and accompanying lipid peroxidation and apoptosis (Chen et al. 1990; Chen et al. 2001; Lash and Anders 1986; Lash et al. 2003; van de Water et al. 1994; van de Water et al. 1995; Xu et al. 2008). In agreement with kidney cells, we recently reported that DCVC increases placental cell ROS generation, lipid peroxidation and mitochondrial-mediated apoptosis in the extravillous trophoblast cell line HTR-8/SVneo (Elkin et al. 2018; Hassan et al. 2016). Taken together, the evidence supports mitochondria as a target and mediator of cytotoxicity in multiple cells types (Lash and Anders 1986).

Flexible and efficient adenosine triphosphate (ATP)-generating mitochondrial function is critical for placental cells because of their sizable energy requirements for carrying out normal biological processes throughout gestation. Specifically, extravillous trophoblast cells require energy for utero-placental invasion, vasculature remodeling and formation of anchoring chorionic villi (Erecinska and Wilson 1982; Fisher et al. 1987; Mando et al. 2014; Vaughan and Fowden 2016). To date, there is considerable evidence supporting the theory that mitochondrial disruptions play a role in the pathophysiology of pregnancy disorders. For example, mitochondria-generated ROS including lipid peroxidation and alterations in mitochondrial DNA content in placental cells have been widely observed in pregnancy disorders involving abnormal placental development, as previously reviewed (Gupta et al. 2005; Holland 7et al. 2017). Based on the importance of the mitochondria in placental cell function and previous studies suggesting that mitochondria are an intracellular target of DCVC toxicity, this study investigated the effects of DCVC on mitochondrial function in a human extravillous trophoblast *in vitro* cell model, HTR-8/SVneo.

## 2. Materials and Methods

### 2.1. Chemicals and reagents

*S*-(1, 2-dichlorovinyl)-L-cysteine (DCVC), a trichloroethylene glutathione conjugation pathway metabolite, was synthesized in powder form by the University of Michigan Medicinal Chemistry Core as previously described (McKinney et al. 1959). High-performance liquid chromatography (HPLC) analysis was used to determine purity (98.7%). A stock solution of 1 mM DCVC was prepared by dissolving DCVC in phosphate buffered saline and stored in small aliquots at −20°C to minimize freeze/thaw cycles. The chemical purity of the DCVC stock solution was confirmed periodically by the core using nuclear magnetic resonance (NMR).

RPMI 1640 culture medium with L-glutamine and without phenol red, 10,000 U/mL penicillin/10,000 μg/mL streptomycin (P/S) solution, and fetal bovine serum (FBS) were purchased from Gibco, a division of Thermo Fisher Scientific (Waltham, MA, USA). Phosphate buffered saline (PBS), Hank's Balanced Salt Solution (HBSS) and 0.25% trypsin were purchased from Invitrogen Life Technologies (Carlsbad, CA, USA). Rotenone,

Author Manuscript Author Manuscript Author Manuscript Author Manuscript

oligomycin, antimycin A and (±)-α-tocopherol were purchased from Sigma-Aldrich (St. Louis, MO, USA). Trifluoromethoxy carbonylcyanide phenylhydrazone (FCCP) was purchased from Cayman Chemical (Ann Arbor, MI, USA). Dimethyl sulfoxide (DMSO) was purchased from Torcis Biosciences (Bristol, UK).

### 2.2. Cell culture and treatment

The HTR-8/SVneo cells were obtained from Dr. Charles H. Graham (Queen's University, Kingston, Ontario, Canada). This cell line was derived from first-trimester human placentae and immortalized with simian virus 40 large T antigen (Graham et al. 1993). The cells have the female genotype of two X chromosomes and express markers of an extravillous trophoblast phenotype. HTR-8/SVneo cells were cultured as previously described (Hassan et al. 2016; Tetz et al. 2013). Briefly, cells were cultured between passages 78–87 in RPMI 1640 medium supplemented with 10% FBS and 1% P/S at 37°C in a 5% CO2 humidified incubator. Cells were sustained in RPMI 1640 growth medium with 10% FBS and 1% P/S prior to and during experiments to ensure optimal cell growth as previously described (Graham et al. 1993). Cells were grown to 70–90% confluence for 24 h after subculture prior to beginning each experiment.

Prior to each experiment, a DCVC stock solution aliquot was quickly thawed in a 37°C water bath and then diluted in RPMI 1640 medium with 10% FBS and 1% P/S to final exposure concentrations of 5–20 μM DCVC. The DCVC concentrations selected for this study are based on a previous study conducted by Lash et al. in which 8 female volunteers were exposed to 100 parts-per-million of TCE, a plausible occupational exposure level, by inhalation. After 4 h of exposure, the female volunteers had an average peak blood concentration of 13.4 μM *S*-(1,2-dichlorovinyl) glutathione, the metabolic precursor to DCVC (Lash et al. 1999). This concentration of DCVG is within the range of the DCVC concentrations used in our study. Additionally, we selected concentrations previously determined to lack overt cytotoxicity in HTR-8/SVneo cells at the times points used in the present study (Elkin et al. 2018; Hassan et al. 2016). In the context of the current study, these concentration thresholds for DCVC toxicity were validated (unpublished results).

### 2.3. Cell line validation

Genomic DNA was extracted from HTR-8/SVneo cells 48 h-post-culture using QIAamp® DNA Mini Kit (Qiagen; Hilden, Germany). Microsatellite genotyping was performed at the University of Michigan DNA Sequencing Core using AmpFLSTR Identifier Plus PCR Amplification Kit run on a 3730XL Genetic Analyzer purchased from Applied Biosystems (Waltham, MA, USA). DNA for 8 tetranucleotide repeat loci and the Amelogenin gender determination marker were identified. The short tandem repeat profile for our cells was compared to the equivalent profile publicly provided by the American Type Culture Collection (ATCC, Manassas, VA, USA) for HTR-8/SVneo (ATCC® CRL-3271™) (ATCC 2015).The following short tandem repeat profile was a perfect match: CSF1PO: 12, D13S317: 9,12, D16S539: 13D5S818: 12, D7S820: 12, TH01: 6,9.3, vWA: 13,18, TPOX: 8, Amelogenin gender determination marker: X (ATCC 2015).

Author Manuscript Author Manuscript Author Manuscript Author Manuscript

### 2.4. Bicinchoninic acid (BCA) assay

Total protein concentration per well was used to normalize bioenergetics experiments. Protein concentrations were measured calorimetrically using the Pierce Bicinchoninic Acid (BCA) Assay Kit (Thermo Fisher Scientific) performed according to the manufacturer's recommended protocol. Briefly, cells were lysed with RIPA lysis buffer. Cell lysates from each sample were transferred to a 96-well clear-bottomed plate, combined with 200 µl working buffer and incubated for 30 minutes at 37°C. Following incubation, protein concentrations were determined with a SpectraMax M2e Multi-Mode Microplate Reader (OD=562 nm) (Molecular Devices) based on comparison to a bovine serum albumin-derived standard curve ranging between 0.0625–2 mg/ml.

### 2.5. Measurement of cellular bioenergetics

We measured changes in cellular bioenergetics using Seahorse XF Analyzer instruments (Agilent; Santa Clara, CA), which allow for simultaneous real-time measurement of the oxygen consumption rate (OCR) and extracellular acidification rate (ECAR) in live cells. We plated HTR-8/SVneo cells at a density of 50,000 cells per well in Seahorse XF Analyzer 24-well plates (Agilent) and allowed the cells to attach for 24 h. Cells were then treated with medium alone (control) or DCVC (10 or 20 µM), 3–5 wells per treatment depending on experiment. We performed mitochondrial stress assays on a Seahorse XF24 Analyzer or an XF24e Analyzer following 6 or 12 h of DCVC exposure, respectively, using the Seahorse XF manufacturer's protocols. During the mitochondrial stress assay, the analyzers took a series of basal OCR and ECAR measurements followed by sequential injections of compounds that target different parts of the electron transport chain: this allowed for the measurement of ATP-linked respiration rate, oxygen-linked maximum respiration rate, non-mitochondrial respiration rate and subsequent calculation of proton leak rate, reserve respiration and acidification rate and coupling efficiency (AgilentSeahorse 2017; Divakaruni et al. 2014). Briefly, the day before the assay, the Seahorse XF cartridge was soaked in Seahorse XF Calibrant (Agilent) and placed in a $CO_2$-free incubator at 37ºC overnight. The day of the assay, the cells in the Seahorse plate were washed twice and cultured in buffer-free RPMI 1640 media (Sigma-Aldrich) containing the appropriate experimental treatments and placed in a $CO_2$-free incubator at 37ºC for 1 h prior to reading. The mitochondrial complex V inhibitor oligomycin (1 µM) was loaded into cartridge injection port A, uncoupler FCCP (1 µM) was loaded into injection port B, and complex I and III inhibitors rotenone and antimycin A (1 µM each) were loaded into injection port C. The cartridge and Seahorse plate were placed in the Seahorse XF24 or XF24e Analyzer and maintained at 37 ºC. The OCR and ECAR were measured using Wave Controller Software version 2.4 (Agilent) at approximately 5-minute intervals, followed by measurements of OCR and ECAR after each injection of an electron transport chain inhibitor. Following the assay, a BCA assay (Thermo Fisher Scientific) was performed to quantify total µg of protein per well for normalization purposes. At least three independent experiments were performed for each time point.

Author Manuscript Author Manuscript Author Manuscript Author Manuscript

### 2.6. Calculation of mitochondrial functional parameters

The bioenergetics parameters were measured or calculated as follows. Non-mitochondrial respiration rate was directly measured by the Seahorse XF Analyzer as the lowest OCR measurement after the rotenone/antimycin A injection. Basal respiration rate is the non-mitochondrial respiration rate subtracted from the last OCR measurement before the first injection. The maximum respiratory rate is the non-mitochondrial respiration rate subtracted from the highest OCR measurement taken after the FCCP injection. Proton leak rate is the non-mitochondrial respiration rate subtracted from the lowest OCR measurement taken after the oligomycin injection. The ATP-linked respiration rate is lowest OCR measurement taken after the oligomycin injection subtracted from the last OCR measurement before the oligomycin injection. The reserve respiration rate is the maximum respiratory rate minus the basal respiration rate. The coupling efficiency is the maximum respiratory rate divided by the basal respiration rate times 100 (AgilentSeahorse 2016). The calculations and relationships of these parameters are visualized in supplemental figure 3.

### 2.7. Measurement of mitochondrial DNA content

Relative mitochondrial DNA content, a proxy for mitochondrial copy number, was estimated by measuring the quantity of genomic DNA of two mitochondrial genes and two nuclear genes and calculating the ratios of mitochondrial DNA to nuclear DNA. HTR-8/SVneo cells were seeded at a density of 400,000 cells per well in a 6-well cell culture plate and allowed to adhere and acclimate for 24 h. Cells were treated with medium alone (control) or DCVC (5, 10 or 20 μM) for 6 or 12 h in separate experiments. Following exposure, DNA was extracted using QIAamp® DNA Mini Kit (Qiagen) following the manufacturer's protocol. Briefly, cells were trypsinized with 0.25% trypsin, transferred to microcentrifuge tubes, centrifuged and resuspended in PBS. Cells were lysed in a assay buffer, centrifuged and washed to remove any remaining cellular debris. The remaining nuclear pellet was lysed with a buffer and treated with proteinase K. The lysate was then filtered through QIAGEN Genomic tip filters to separate genomic DNA. Following filtration, the genomic DNA was washed, eluted and stored at −80 ºC in 10 mM Tris-Cl buffer with a pH of 8.5.

Following DNA extraction, quantitative real-time PCR (qRT-PCR) was performed on the genomic DNA using a commercially available Human Mitochondrial DNA (mtDNA) Monitoring Primer Set (Takara Bio; Mountain View, CA) containing primers for two nuclear encoded genes; *SLCO2B1*and *SERPINA1* and two mitochondrial encoded gene: *ND1* and *ND5*. real-time PCR reactions were prepared with SYBR Green Mastermix (Qiagen SABiosciences; Sioux Falls, SD, USA) and commercially purchased primers and run on a Bio-Rad (Hercules, CA) CFX96 Real Time C1000 \thermal cycler following the manufacturer's recommended protocols.

The mitochondrial content was calculated using the manufacturer's recommended procedure (Takara 2013a). Briefly, the difference in the Ct values for the *ND1/SLCO2B1* pair and *ND5/SERPINA1* was calculated separately). The $2^{\Delta Ct}$ for ΔCt1 and ΔCt2 were calculated. The mean of the two $2^{\Delta Ct}$ values was used as mitochondrial content for each DCVC exposure (Takara 2013a, b). The experiment was replicated three times for the 6-h time point

Author Manuscript Author Manuscript Author Manuscript Author Manuscript

and four times for 12-h time point. Gene expression was measured in technical duplicate by qRT-PCR.

### 2.8. Measurement of mitochondrial membrane potential

To measure relative mitochondrial membrane potential, HTR-8/SVneo cells were seeded at a density of 20,000 cells in each well in a black, clear-bottomed plate and allowed to adhere for 24 h. After acclimation, cells were treated with medium alone (control), DCVC (5, 10, and 20 μM), or 10 μM FCCP (positive control) in quintuplicate for 3, 6, 9 or 12 h. Relative changes in the mitochondrial membrane potential were measured using the TMRE Mitochondrial Membrane Potential Assay Kit (Cayman Chemical). Because the fluorochrome tetramethylrhodamine ethyl ester (TMRE) selectively accumulates in mitochondria with normal polarized membrane potentials, the number of healthy mitochondria is proportional to TMRE fluorescence intensity (Crowley et al. 2016). The assay was performed using the manufacturer's recommended protocol with some modification, as follows. Cells were loaded with the fluorochrome by incubation with 125 nM TMRE diluted in HBSS (Thermo Fisher Scientific) at room temperature for 15 minutes followed by incubation at 37ºC for 30 minutes. Following incubation, cells were washed 3 times with HBSS and left to equilibrate to room temperature for 15 minutes. TMRE fluorescence intensity (excitation/emission=530/580 nm) was measured using a SpectraMax M2e Multi-Mode Microplate Reader (Molecular Devices). Three independent experiments were performed for each time point.

### 2.9. Visualization of changes in mitochondrial membrane potential

Fluorescence microscopy was used to visualize the effect of DCVC on relative mitochondrial membrane potential. HTR-8/SVneo cells were seeded at a density of 400,000 cells per well in a 6-well clear bottom plate and allowed to adhere for 24 h. Cells were then treated with medium alone (control) or DCVC (10 or 20 μM) for 12 h. Cells were loaded with TMRE as previously described. Additionally, cellular nuclei were stained with Hoechst dye (Thermo Fisher Scientific). Cells were viewed and images were captured using an EVOS FL digital inverted fluorescence microscope (Thermo Fisher Scientific). TMRE fluorescence was visualized in the RFP fluorescence channel and Hoechst stain was visualized in the DAPI fluorescence channel. Photo images were then merged to create final images using EVOS FL software.

### 2.10. Treatment with (±)-α-tocopherol to assess modulation of DCVC-induced changes in mitochondrial function

The ability of (±)-α-tocopherol to attenuate DCVC-induced perturbation of mitochondrial bioenergetics and mitochondrial membrane potential were measured using the Seahorse XF Analyzer and TMRE fluorescence, respectively. For the Seahorse XF Analyzer experiments, cells were seeded at a density of 50,000 per well (previously determined by cell density-OCR experiments), in a Seahorse XF24 Analyzer 24-well plate. For the TMRE fluorescence experiment, cells were seeded at a density of 20,000 cells per well in a 96-well black, clear-bottom plate and allowed to adhere for 24 h. To initiate treatment, cells were incubated for 15 min with 50 μM (±)-α-tocopherol, a concentration previously demonstrated to attenuate DCVC-stimulated caspase 3+7 activity in HTR-8/SVneo cells (Elkin et al. 2018). Then,

Author Manuscript Author Manuscript Author Manuscript Author Manuscript

cells were treated with 0.01% DMSO (solvent control for α-tocopherol), (±)-α-tocopherol (50 μM), DCVC (20 μM), or DCVC (20 μM) plus (±)-α-tocopherol (50 μM). After 12 h of exposure, mitochondrial bioenergetics was measured with the Seahorse XF Analyzer and membrane potential depolarization was measured by TMRE fluorescence intensity, as previously described.

### 2.11. Statistical analysis

All experiments were performed independently and repeated three to four times. When applicable, technical replicates were averaged within each experiment. Data collected together from time-course experiments were analyzed using two-way analysis of variance (ANOVA), followed by Tukey's post-hoc test for comparison of means. Data collected from experiments conducted separately using different exposure times were analyzed by adjusted linear mixed-models with posthoc Tukey multiple comparisons. These comparisons were restricted to within each time point tested, as indicated by vertical dashed line on respective graphs, were applicable. Two-way ANOVA followed by Tukey's post-hoc comparison of means were performed with GraphPad Prism software version 7 (GraphPad Software Inc., San Diego, CA, USA). Adjusted linear mixed-models with posthoc Tukey multiple comparisons were performed with SPSS experiments were conducted separately software version 22 (IBM, Armonk, New York, USA). Data are expressed as means ± SEM. N=number of independent experiments. $P < 0.05$ was considered statistically significant in all experiments.

## 3. Results

### 3.1. DCVC effects on cellular bioenergetics and mitochondrial function

Because DCVC decreases mitochondrial respiration in human and rat renal proximal tubular cells (Lash and Anders 1987; Lash et al. 2001; Lash et al. 2003; Xu et al. 2008), Seahorse XF Analyzer instruments were used to assess mitochondrial OCR perturbations in HTR-8/SVneo cells (Fig. 1) (AgilentSeahorse 2017; Divakaruni et al. 2014). Concomitantly, the instrument also assessed DCVC-induced changes in the extracellular acidification rate. Overall ECAR and OCR profiles for the initial 130 minutes directly following treatment with medium alone (control), 10 μM DCVC, or 20 μM DCVC for 6 and 12 h are displayed in figures 1A and 1C, respectively. Furthermore, functional parameters are individually displayed in figures 1Bi and 1Di–vi, respectively.

**3.1.1. Extracellular acidification rate—**DCVC-induced increases in the basal ECAR were detected after 6 and 12 h of exposure (Fig. 1B). After 6 h of exposure, basal ECAR measurements significantly increased 26% and 63% with 10 and 20 μM DCVC, respectively, compared to time-matched controls (Fig 1Bi; $P<0.05$). In contrast, DCVC significantly increased basal ECAR by 37% only after 12 h of exposure to 20 μM DCVC (Fig 1Bi; $P=0.01$). No significant effects were observed in ECAR measured in real-time for the first 90 minutes immediately following DCVC treatment (Sup. Fig. 1). Interestingly, although the bioenergetics studies conducted at 6 or 12 h-post DCVC exposure were separate and treated as such, we also observed lower mean basal ECAR in non-treated cells

Author Manuscript Author Manuscript Author Manuscript Author Manuscript

measured after 12 h compared to 6 h. Although not directly caused by mitochondrial perturbations, changes in ECAR may be connected indirectly to mitochondrial dysfunction.

**3.1.2. Mitochondrial oxygen consumption rate—**Concordant with elevated ECAR, treatment with 10 and 20 μM DCVC for 6 or 12 h significantly altered multiple OCR parameters after one or both time points (Fig. 1D). Basal OCR increased 38% with 20 μM DCVC after 6 h (Fig. 1Di; P=0.025), but the opposite effect – decreased basal OCR by 57% – was observed after 12 h of DCVC exposure, compared to time-matched controls (Fig. 1Di; P=0.025). Although the maximum OCR was not impacted by DCVC treatment after 6 h, it decreased after 12 h by 45% and 64% with 10 μM and 20 μM DCVC treatment, respectively, compared to time-matched controls (Fig. 1Dii; P<0.0001). On the other hand, reserve OCR declined significantly at both time points: 72% with 20 μM after 6 h (P=0.009), and 55% and 73% with 10 μM or 20 μM DCVC treatment, respectively, after 12 h (P<0.0001), compared to time-matched controls (Fig. 1Diii). Proton leak was significantly elevated 60% with 10 and 20 μM DCVC treatment for 6 h (P<0.0001), however, it was only elevated 32% with 10 μM DCVC treatment following 12 h of exposure (P=0.02), compared to time-matched controls (Fig. 1Div). Despite no change in the ATP-linked OCR after 6 h of DCVC exposure, the rate declined significantly 42% and 82% with 10 and 20 μM DCVC, respectively, after 12 h of exposure, compared to time-matched controls (Fig. 1Dv; P<0.002). Lastly, ATP coupling efficiency decreased significantly by 40% and 48% with 10 and 20 μM DCVC treatment, respectively, after 6 h of exposure (P<0.0001), and by 24% and 58% with 10 and 20 μM DCVC treatment, respectively, after 12 h of exposure (P<0.002), compared to time-matched controls (Fig. 1Dvi). No significant effects were observed in OCR measured in real-time for the first 90 minutes following treatment with DCVC (Sup. Fig. 1). In addition, the non-mitochondrial OCR was not was not significantly affected by DCVC treatment at 12 h, however it was significantly reduced after 6 h with 20 μM (Sup. Fig. 2). Lastly, like the ECAR, we also observed lower mean basal OCAR in non-treated cells measured after 12 h compared to 6 h. Taken together, these results indicate that DCVC exposure between 6 and 12 h caused progressive changes to mitochondrial function. However, as with ECAR, DCVC treatment did not exert immediate effects on the OCR in placental cells.

### 3.2. Effect of DCVC on mitochondrial DNA content

Because mitochondria are primary targets that mediate DCVC-induced cytotoxicity in another cell type (Lash and Anders 1986), mitochondrial DNA content was measured as a proxy for mitochondrial copy number in the HTR-8/SVneo cells. Exposure to 20 μM DCVC for 12 h reduced mitochondrial DNA content by 30% compared to time-matched controls (Fig. 2; P=0.02). There were no significant differences in the mitochondrial DNA content with 10 μM DCVC at 12 h, nor with 10 and 20 μM DCVC at 6 h, compared to time-matched controls. The results indicate a modest decline in mitochondrial content that required at least 12 h of exposure to 20 μM DCVC.

### 3.3. Effect of DCVC on relative mitochondrial membrane potential

To further assess the impact of DCVC on mitochondrial function, the TMRE fluorochrome was used to examine DCVC-induced changes to mitochondrial membrane potential. DCVC

Author Manuscript Author Manuscript Author Manuscript Author Manuscript

treatment decreased the TMRE fluorescence signal in time-and concentration-dependent manners (no significant interaction detected between time and treatment, Fig. 3A; P=0.1533). Treatment with 20 μM DCVC for 12 h stimulated a 64% decline of fluorescence compared to time-matched controls (P=0.0013), as well as decreased fluorescence compared to other DCVC concentrations at 12 h (P<0.002) and earlier exposure durations with 20 μM DCVC (Fig. 3A; P<0.001). No other significant DCVC-induced changes in mitochondrial membrane potential were detected. Fluorescence microscopy with TMRE and Hoechst nuclear stain provided visual confirmation of these results (Fig. 3Bi–iii). These results demonstrate that the mitochondrial membrane remained polarized for at least 9 h during exposure to 20 μM DCVC, with depolarization onset between 9 and 12 h of exposure. These results suggest an exposure duration threshold of 12 h for 20 μM DCVC-induced mitochondrial membrane depolarization.

### 3.4. Effect of antioxidant co-treatment on relative mitochondrial membrane potential depolarization and decline in oxygen consumption rate

Due to evidence of reactive oxygen species and lipid peroxidation involvement in the toxicological mechanism for DCVC-mediated toxicity in placental and kidney cells (Beuter et al. 1989; Chen et al. 1990; Elkin et al. 2018; Groves et al. 1991; Hassan et al. 2016), the role of lipid peroxidation in DCVC-induced mitochondrial perturbations was evaluated by including treatment with (±)α-tocopherol, an antioxidant that blocks lipid peroxidation (Horwitt 1986). Co-treatment with 50 μM (±)α-tocopherol significantly rescued mitochondrial membrane depolarization caused by 20 μM DCVC exposure for 12 h (Fig. 4A; P < 0.001). However, (±)α-tocopherol co-treatment did not attenuate the DCVC-induced decreases in OCR, ATP-linked OCR, maximum OCR and ATP coupling efficiency (Figs. 4Bi–iv). These results indicate that lipid peroxidation may mediate DCVC-induced depolarization of the mitochondrial membrane. However, the inability of (±)α-tocopherol to prevent DCVC-induced decrease in basal OCR may suggest that DCVC-induced lipid peroxidation does not initiate mitochondrial dysfunction but rather results from it.

## 4. Discussion

Several studies report associations between maternal TCE exposure and increased risk of adverse birth outcomes (Forand et al. 2012; Ruckart et al. 2014). Additionally, our laboratory reported pregnancy-related TCE toxicity in Wistar rats with oxidative stress impacts on the placenta (Loch-Caruso et al. 2018). Still, the mechanism of TCE-mediated toxicity in pregnancy remains poorly characterized. Here, we examined the effects of the TCE glutathione conjugation-derived metabolite *S*-(1, 2-dichlorovinyl)-L-cysteine on the mitochondria of placental cells.

The assessment of mitochondrial bioenergetics in HTR-8/SVneo cells revealed that treatment with 20 μM DCVC for 6 h significantly elevated the basal OCR compared to controls, whereas the same DCVC concentration had the opposite effect of depressing basal OCR after 12 h. Because previous studies demonstrated that 20 μM DCVC treatment was not cytolethal after 12 h, yet apoptotic caspase activity increased after 12 h (Elkin et al. 2018; Hassan et al. 2016), the previous findings and the OCR results presented here likely

Author Manuscript Author Manuscript Author Manuscript Author Manuscript

reflect initial metabolic compensation occurring after 6 h of DCVC exposure that transitioned to a pathological process after approximately 12 h of DCVC exposure. Furthermore, the current study measured no change in mitochondrial OCAR or ECAR during the first 90 minutes of real-time exposure to DCVC (Sup. Fig. 1), supporting the theory of an initial compensatory mechanism for maintaining metabolic homeostasis preceding pathological consequences.

To our knowledge, this is the first report of DCVC-stimulated OCR elevation followed by depression in any cell type. Prior studies conducted with renal proximal tubular cells reported DCVC-induced decreases in mitochondrial OCR at earlier time points: 15 minutes with 1 mM DCVC (Lash and Anders 1986) and 1 h with 10 μM DCVC (Xu et al. 2008). The increased time required for DCVC-induced mitochondrial disruption in HTR-8/SVneo cells compared to renal proximal tubular cells may be attributed to cell-specific variations in transport, metabolism and/or accumulation of DCVC, resulting in the ability of HTR-8/SVneo cells to initially compensate for DCVC exposure, unlike proximal tubular cells. For example, because the toxicity of DCVC is likely dependent on the expression and activity of the downstream biotransforming enzyme beta-lyase (Lash et al. 2014; Lash et al. 2000a), differing levels of beta-lyase expression and/or activity may be one explanation for why kidney cells appear to be more sensitive to DCVC treatment than placental cells. Regardless, our results indicate that DCVC disrupted mitochondrial basal OCR in HTR-8/SVneo cells, contributing novel evidence of mitochondrial involvement for DCVC-induced placental cell dysfunction.

Our bioenergetics experiments revealed for the first time that DCVC compromised cellular bioenergetic capacity. Following 6 h of DCVC exposure, unchanged maximum OCR, elevated basal OCR and resulting diminished reserve OCR revealed that the HTR-8/SVneo cells were operating closer to their bioenergetic limit compared to non-treated cells. The maximum OCR reflects the top achievable mitochondrial respiration rate (Pereira et al. 2014), whereas spare OCR describes the cells' ability to adaptively elevate the OCR in response to increased energy demand (Brand and Nicholls 2011). These results support a compensatory process occurring at 6 h, likely due to increased energy demand in response to DCVC exposure. Furthermore, exposure to 10 and 20 μM DCVC for 6 h substantially elevated proton leak, the movement of proton back across the mitochondrial inner membrane into the matrix independent of ATP synthase. Although this process may occur under pathological conditions, physiological regulation of proton leak through mitochondrial inner membrane integral proteins occurs as both a signaling/regulatory mechanism and an adaptive process (Cheng et al. 2017; Jastroch et al. 2010). Indeed, induced proton leak resulting in uncoupling has been suggested as a protective mechanism to limit excessive ROS generation during elevated oxidative phosphorylation (Brookes 2005), a scenario consistent with the DCVC response we observed at 6 h in the present study. Thus, although further investigation is warranted, the evidence, suggests that mitochondrial compensation occurred in response to DCVC exposure for 6 h in HTR-8/SVneo cells.

Contrary to the mitochondria functional parameters measured 6 h-post DCVC treatment, continuous DCVC exposure for 12 h decreased basal, maximum and spare OCRs, indicating a drop in cellular bioenergetic capacity and limiting mitochondrial-mediated cellular

Author Manuscript Author Manuscript Author Manuscript Author Manuscript

adaptability. These results are consistent with our previous study showing elevated caspase activity in the absence of detectable cell death 12 h-post DCVC exposure (Elkin et al. 2018). Consequently, the results likely indicate a critical transition to a pathological process in which mitochondria lose their ability to compensate and initiate a decline in cellular function leading to cell death. Notably, other studies have also reported diminished spare and/or maximum OCR in pre-eclamptic placental tissue (Holland et al. 2018), or in HTR-8/SVneo cells treated with maternal serum from pregnancies complicated with pre-eclampsia compared to normal pregnancies (Sanchez-Aranguren et al. 2018). Taken together, these findings suggest that DCVC may disrupt oxidative phosphorylation and diminish mitochondrial adaptability over time as a possible mechanism by which TCE exposure promotes placental toxicity.

Interestingly, although the bioenergetics studies conducted after 6 or 12 h of DCVC exposure were separate experiments and treated as such in our data analysis and interpretation, we also observed lower mean basal OCAR and ECAR in non-treated cells measured after 12 h compared to 6 h. This observation may be attributed to differences in the length of time in cell culture reflecting an overall slow-down in the metabolic rate of the cells or the atypical culture conditions required to perform the mitochondrial stress assay. Nevertheless, the OCR and ECAR rates and DCVC-induced changes measured over the course of multiple experiments were relatively consistent within each time point, as demonstrated by appropriate normalization and statistical analyses.

In addition to mitochondrial bioenergetics, we demonstrated that 20 μM DCVC depolarized the mitochondrial membrane after 12 h of exposure, a finding consistent with multiple DCVC toxicity studies in kidney cells across different species (Chen et al. 2001; Lash and Anders 1987; van de Water et al. 1994; Xu et al. 2008). Because 6 h exposure to DCVC increased mitochondrial proton leak and decreased ATP coupling efficiency, yet mitochondrial membrane depolarization did not occur until after 12 h of exposure, elevated proton leak and ATP uncoupling preceded mitochondrial membrane depolarization (Divakaruni and Brand 2011). Indeed, as demonstrated here and by others (Heiskanen et al. 1999), evidence supports mitochondrial membrane depolarization as a later event in the sequence of progressive mitochondrial injury. Because development of mitochondrial membrane depolarization required 12 h of DCVC exposure, the data support the theory of an adaptive process occurring at 6 h with a subsequent pathological process developing and manifesting around 12 h in HTR-8/SVneo cells. This finding not only demonstrates the central role of the mitochondria in DCVC-induced placental cytotoxicity, it also aids in elucidating the specific sequence of events comprising DCVC-induced adaptability and subsequent pathogenesis of mitochondrial injury.

Consistent with our previous studies demonstrating a protective role for the antioxidant (±)-α-tocopherol in DCVC-induced cytotoxicity (Elkin et al. 2018; Hassan et al. 2016), we demonstrated that (±)-α-tocopherol attenuated DCVC-induced mitochondrial membrane depolarization after 12 h. The most well-established antioxidant function of (±)-α-tocopherol is to block lipid peroxidation, the production of lipid peroxyl radicals resulting from oxidation of lipid molecules by ROS species (Burton and Ingold 1981; Traber and Atkinson 2007). Consequently, although levels of lipid peroxides were not directly tested

Author Manuscript Author Manuscript Author Manuscript Author Manuscript

here, our results suggest that DCVC-stimulated mitochondrial membrane depolarization may be dependent on lipid peroxidation based on (±)-α-tocopherol attenuation. Indeed, DCVC-induced lipid peroxidation has been directly measured by us in HTR-8/SVneo cells (Elkin et al. 2018) and by other researchers in kidney proximal tubular cells (van de Water et al. 1994). Moreover, the present study showed that 12-h (±)α-tocopherol co-treatment failed to rescue DCVC-induced impairment of OCR parameters, suggesting that the observed OCR disruptions were independent of lipid peroxidation. Combined, these findings suggest that the DCVC-induced OCR perturbations may have increased ROS generation and subsequent lipid peroxidation, culminating in mitochondrial membrane depolarization. In this scenario, mitochondria may serve as both a source and target of ROS generation in DCVC-induced cytotoxicity (Zorov et al. 2000; Zorov et al. 2014). Collectively, these findings contribute evidence to the sequence of DCVC-induced mitochondrial pathogenesis and may suggest the involvement of lipid peroxidation in the mechanism of DCVC toxicity. In this proposed scenario, mitochondria may serve as both a source and target of ROS generation in DCVC-induced cytotoxicity (Zorov et al. 2000; Zorov et al. 2014).

Additionally, DCVC treatment for 12 h reduced mitochondrial DNA content in HTR-8/SVneo cells. To our knowledge, no other studies have reported similar findings related to DCVC toxicity, despite extensive evidence of mitochondrial involvement in DCVC-mediated toxicity in other cell types. However, studies have shown a relationship between mitochondrial DNA content and placental impairment (Holland et al. 2017). Mitochondrial DNA content was found to be decreased in placental tissue (Diaz et al. 2014; Poidatz et al. 2015) and cytotrophoblasts (Mando et al. 2014) isolated from pregnancies complicated with intrauterine growth restriction or small for gestational age. In contrast, other studies reported higher mitochondrial DNA content in placenta from intrauterine growth restricted-pregnancies (Lattuada et al. 2008; Mando et al. 2014). Nevertheless, the weight of evidence supports a role for altered placental mitochondrial DNA content in pregnancy disorders with placental dysfunction, despite the need for further clarification. Consequently, our finding contributes to evidence of mitochondrial involvement in DCVC-induced placental disruption.

In the current study, we observed an increase in extracellular acidification with both 6 and 12 h of DCVC exposure, likely indicating intracellular pH fluctuations. Although not directly caused by mitochondrial perturbations, ECAR alterations may be related to mitochondrial function indirectly through changes in cellular energy metabolism. For example, elevated amino acid flux may increase extracellular acidification. Indeed, we recently generated evidence that DCVC treatment for 6 and 12 h caused a compensatory increase of intracellular concentrations of energy-relevant amino acids, likely used for energy metabolism as alternative biofuel for ATP production (unpublished results). Although not directly investigated, ECAR perturbations may be a secondary effect of changes in energy metabolism and related mitochondrial functioning.

We used DCVC concentrations relevant to potential human occupational exposure levels to TCE, the parent compound for DCVC in vivo. The U.S. Occupational Safety and Health Administration Permissible Exposure Limit (PEL) for TCE is 100 ppm averaged over an 8-hour work day (OSHA 2019). Female volunteers exposed to 100 ppm of TCE for 4 h by

Author Manuscript Author Manuscript Author Manuscript Author Manuscript

inhalation had an average peak blood concentration of 13.4 μM *S*-(1,2-dichlorovinyl) glutathione, the metabolic precursor to DCVC (Lash et al. 1999). This peak DCVC blood concentration is encompassed within the range of concentrations used in our study. Moreover, a second study detected TCE concentrations up to 229 ppm, more than twice the PEL, in 80 exposed workers (29% women) wearing personal aerosolized monitoring devices (Walker et al. 2016). Thus, our study contributes valuable evidence of the effects of plausible DCVC concentrations in human placental cells and possibly other cell types.

The present study used HTR-8/SVneo cells, an immortalized extravillous trophoblast cell line. These cells express a combination of molecular markers and functional characteristics that are unique to extravillous trophoblasts (Damsky et al. 1994; Graham et al. 1994; Graham et al. 1993; Irving et al. 1995; Khan et al. 2011; Kilburn et al. 2000; Zdravkovic et al. 1999). Some recent reports concluded that the HTR-8/SVneo cell line contains mixed populations of cells (Abou-Kheir et al. 2017; Takao et al. 2011): however, no efforts were made to verify the identity of the cell line in these studies. In contrast, we obtained our cells from the lab of origin of the cell line and used Sanger sequencing to validate our HTR-8/SVneo cells. Overall, our *in vitro* experiments do not reflect the complicated *in vivo* dynamics, and further studies in other models are needed to confirm our results.

### 4.1 Conclusion

In summary, we present evidence detailing a partial sequence of events leading to DCVC-induced adaptive and subsequently pathogenic changes in the mitochondria of HTR-8/SVneo cells. The evidence suggests that DCVC caused progressive mitochondrial OCR perturbations resulting in mitochondrial membrane depolarization (Fig. 5). To our knowledge, our study is the first to report that DCVC induced mitochondrial effects on placental cells. Our findings contribute to the biological plausibility of DCVC-induced placental toxicity, indicating that investigation is warranted.

## Supplementary Material

Refer to Web version on PubMed Central for supplementary material.

## Acknowledgments

We thank Sydney Bridges of the Nutrition Obesity Research Center for assistance with early Seahorse experiments and Larisa Yeomans of the University of Michigan Biochemical Nuclear Magnetic Resonance Core for verifying the chemical structure of DCVC. Finally, we gratefully acknowledge Sean Harris, PhD, Anthony Su, Faith Bjork, JeAnna Redd and Molly Mulcahy for assistance with learning new laboratory techniques and for helpful scientific discussions, and Monica Smolinski for assistance with BCA assays.

Funding Information

This work was supported by the United States National Institute of Environmental Health Sciences, National Institutes of Health (grant numbers P42 ES0171982, P30 ES017885, and T32 ES007062), the United States National Institute of Diabetes and Digestive Kidney Diseases (grant numbers R01 DK107535 and P30 DK089503); and The University of Michigan. The content is solely the responsibility of the authors and does not necessarily represent the official views of the NIEHS, NIH or the University of Michigan.

Author Manuscript Author Manuscript Author Manuscript Author Manuscript

## Abbreviations:

| | |
|---|---|
| **ANOVA** | analysis of variance |
| **ATCC** | American Type Culture Collection |
| **ATP** | adenosine triphosphate |
| **BCA** | bicinchoninic Acid |
| **DCVC** | S-(1, 2-dichlorovinyl)-L-cysteine |
| **DMSO** | Dimethyl sulfoxide |
| **ECAR** | extracellular acidification rate |
| **FBS** | fetal bovine serum |
| **FCCP** | trifluoromethoxy carbonylcyanide phenylhydrazone |
| **HBSS** | Hank's Balanced Salt Solution |
| **HPLC** | high-performance liquid chromatography |
| **ND1** | NADH dehydrogenase 1 |
| **ND5** | NADH dehydrogenase 5 |
| **NMR** | nuclear magnetic resonance |
| **NTP** | National Toxicology Program |
| **OSHA** | Occupational Safety and Health Administration |
| **OCR** | oxygen consumption rate |
| **PBS** | phosphate buffered saline |
| **PEL** | Permissible Exposure Limit ppm, parts-per-million |
| **P/S** | penicillin/streptomycin |
| **ROS** | reactive oxygen species |
| **SERPINA1** | Serpin Family A Member 1 |
| **SLCO2B1** | Solute Carrier Organic Anion Transporter Family Member 2B1 |
| **TCE** | trichloroethylene |
| **TMRE** | fluorochrome tetramethylrhodamine ethyl ester |

## References

Abou-Kheir W, Barrak J, Hadadeh O. and Daoud G. 2017 HTR-8/SVneo cell line contains a mixed population of cells. Placenta 50, 1–7. [PubMed: 28161053]

Author Manuscript Author Manuscript Author Manuscript Author Manuscript

AgilentSeahorse. 2016 Multi-File XF Report Generator User Guide. Agilent Seahorse 103312–400 Rev E.

AgilentSeahorse. 2017 Seahorse XF Cell Mito Stress Test Kit User Guide. Agilent Technologies.

ATCC. 2015 American Type Culture Collection Product Sheet: HTR8/SVneo (ATCC® CRL3271™). American Type Culture Collection.

Ayala A, Munoz MF and Arguelles S. 2014 Lipid peroxidation: production, metabolism, and signaling mechanisms of malondialdehyde and 4-hydroxy-2-nonenal. Oxid Med Cell Longev 2014, 360438.

Beuter W, Cojocel C, Muller W, Donaubauer HH and Mayer D. 1989 Peroxidative damage and nephrotoxicity of dichlorovinylcysteine in mice. J Appl Toxicol 9, 181–186. [PubMed: 2745925]

Brand MD and Nicholls DG 2011 Assessing mitochondrial dysfunction in cells. The Biochemical journal 435, 297–312. [PubMed: 21726199]

Brookes PS 2005 Mitochondrial H(+) leak and ROS generation: an odd couple. Free Radic Biol Med 38, 12–23. [PubMed: 15589367]

Burton GJ and Fowden AL. 2015 The placenta: a multifaceted, transient organ. Philos Trans R Soc Lond B Biol Sci 370, 20140066.

Burton GW and Ingold KU 1981 Autoxidation of biological molecules. 1. The antioxidant activity of vitamin E and related chain-breaking phenolic antioxidants in vitro. Journal of the American Chemical Society 103, 6472–6477.

Chen Q, Jones TW, Brown PC and Stevens JL. 1990 The mechanism of cysteine conjugate cytotoxicity in renal epithelial cells. Covalent binding leads to thiol depletion and lipid peroxidation. J Biol Chem 265, 21603–21611.

Chen Y, Cai J, Anders MW, Stevens JL and Jones DP 2001 Role of mitochondrial dysfunction in S-(1,2-dichlorovinyl)-l-cysteine-induced apoptosis. Toxicol Appl Pharmacol 170, 172–180. [PubMed: 11162782]

Cheng J, Nanayakkara G, Shao Y, Cueto R, Wang L, Yang WY, Tian Y, Wang H. and Yang X. 2017 Mitochondrial Proton Leak Plays a Critical Role in Pathogenesis of Cardiovascular Diseases. Adv Exp Med Biol 982, 359–370. [PubMed: 28551798]

Cichocki JA, Guyton KZ, Guha N, Chiu WA, Rusyn I. and Lash LH 2016 Target Organ Metabolism, Toxicity, and Mechanisms of Trichloroethylene and Perchloroethylene: Key Similarities, Differences, and Data Gaps. J Pharmacol Exp Ther 359, 110–123. [PubMed: 27511820]

Crowley LC, Christensen ME and Waterhouse NJ 2016 Measuring Mitochondrial Transmembrane Potential by TMRE Staining. Cold Spring Harb Protoc 2016.

Damsky CH, Librach C, Lim KH, Fitzgerald ML, McMaster MT, Janatpour M, Zhou Y, Logan SK and Fisher SJ 1994 Integrin switching regulates normal trophoblast invasion. Development 120, 3657–3666. [PubMed: 7529679]

Darnerud PO, Brandt I, Feil VJ and Bakke JE 1989 Dichlorovinyl cysteine (DCVC) in the mouse kidney: tissue-binding and toxicity after glutathione depletion and probenecid treatment. Arch Toxicol 63, 345–350. [PubMed: 2818197]

Davies EL., Bell JS and Bhattacharya S. 2016 Preeclampsia and preterm delivery: A population-based case-control study. Hypertens Pregnancy 35, 510–519. [PubMed: 27322489]

Diaz M, Aragones G, Sanchez-Infantes D, Bassols J, Perez-Cruz M, de Zegher F, Lopez-Bermejo A. and Ibanez L. 2014 Mitochondrial DNA in placenta: associations with fetal growth and superoxide dismutase activity. Horm Res Paediatr 82, 303–309. [PubMed: 25247554]

Divakaruni AS and Brand MD 2011 The regulation and physiology of mitochondrial proton leak. Physiology (Bethesda) 26, 192–205. [PubMed: 21670165]

Divakaruni AS, Paradyse A, Ferrick DA, Murphy AN and Jastroch M. 2014 Analysis and interpretation of microplate-based oxygen consumption and pH data. Methods Enzymol 547, 309–354. [PubMed: 25416364]

Elkin ER, Bridges D. and Loch-Caruso R. 2019 The trichloroethylene S-(1,2-Dichlorovinyl)-L-cysteine causes an arly metabolic shift followed by mitochondrial dysfunction in a frst trimester extravillous trophoblast cell line. The Toxicologist: Supplement to Toxicological Sciences.

Elkin ER, Harris SM and Loch-Caruso R. 2018 Trichloroethylene metabolite S-(1,2-dichlorovinyl)-l-cysteine induces lipid peroxidation-associated apoptosis via the intrinsic and extrinsic apoptosis

Author Manuscript Author Manuscript Author Manuscript Author Manuscript

pathways in a first-trimester placental cell line. Toxicol Appl Pharmacol 338, 30–42. [PubMed: 29129777]

Erecinska M. and Wilson DF 1982 Regulation of cellular energy metabolism. J Membr Biol 70, 1–14. [PubMed: 6226798]

Fisher GJ, Kelley LK and Smith CH 1987 ATP-dependent calcium transport across basal plasma membranes of human placental trophoblast. Am J Physiol 252, C38–46. [PubMed: 2949624]

Forand SP, Lewis-Michl EL. and Gomez MI. 2012 Adverse birth outcomes and maternal exposure to trichloroethylene and tetrachloroethylene through soil vapor intrusion in New York State. Environ Health Perspect 120, 616–621. [PubMed: 22142966]

Goodman DR, James RC and Harbison RD 1982 Placental toxicology. Food Chem Toxicol 20, 123–128. [PubMed: 7040181]

Graham CH, Connelly I, MacDougall JR, Kerbel RS, Stetler-Stevenson WG and Lala PK 1994 Resistance of malignant trophoblast cells to both the anti-proliferative and anti-invasive effects of transforming growth factor-beta. Experimental cell research 214, 93–99. [PubMed: 8082752]

Graham CH, Hawley TS, Hawley RG, MacDougall JR, Kerbel RS, Khoo N. and Lala PK 1993 Establishment and characterization of first trimester human trophoblast cells with extended lifespan. Experimental cell research 206, 204–211. [PubMed: 7684692]

Groves CE, Lock EA and Schnellmann RG 1991 Role of lipid peroxidation in renal proximal tubule cell death induced by haloalkene cysteine conjugates. Toxicol Appl Pharmacol 107, 54–62. [PubMed: 1987660]

Guha N, Loomis D, Grosse Y, Lauby-Secretan B, El Ghissassi F, Bouvard V, Benbrahim-Tallaa L, Baan R, Mattock H, Straif K. and International Agency for Research on Cancer Monograph Working, G. 2012 Carcinogenicity of trichloroethylene, tetrachloroethylene, some other chlorinated solvents, and their metabolites. Lancet Oncol 13, 1192–1193. [PubMed: 23323277]

Hassan I, Kumar AM, Park HR, Lash LH and Loch-Caruso R. 2016 Reactive Oxygen Stimulation of Interleukin-6 Release in the Human Trophoblast Cell Line HTR-8/SVneo by the Trichlorethylene Metabolite S-(1,2-Dichloro)-l-Cysteine. Biology of reproduction 95, 66. [PubMed: 27488030]

Heiskanen KM, Bhat MB, Wang HW, Ma J. and Nieminen AL. 1999 Mitochondrial depolarization accompanies cytochrome c release during apoptosis in PC6 cells. J Biol Chem 274, 5654–5658. [PubMed: 10026183]

Holland OJ, Cuffe JSM, Dekker Nitert M, Callaway L, Kwan Cheung KA, Radenkovic F. and Perkins AV 2018 Placental mitochondrial adaptations in preeclampsia associated with progression to term delivery. Cell Death Dis 9, 1150. [PubMed: 30455461]

Horwitt MK 1986 The promotion of vitamin E. J Nutr 116, 1371–1377. [PubMed: 3528433]

Ilekis JV, Tsilou E, Fisher S, Abrahams VM, Soares MJ, Cross JC, Zamudio S, Illsley NP, Myatt L, Colvis C, Costantine MM, Haas DM, Sadovsky Y, Weiner C, Rytting E. and Bidwell G. 2016 Placental origins of adverse pregnancy outcomes: potential molecular targets: an Executive Workshop Summary of the Eunice Kennedy Shriver National Institute of Child Health and Human Development. Am J Obstet Gynecol 215, S1–S46. [PubMed: 26972897]

Irving JA, Lysiak JJ, Graham CH, Hearn S, Han VK and Lala PK 1995 Characteristics of trophoblast cells migrating from first trimester chorionic villus explants and propagated in culture. Placenta 16, 413–433. [PubMed: 7479613]

Jastroch M, Divakaruni AS, Mookerjee S, Treberg JR and Brand MD 2010 Mitochondrial proton and electron leaks. Essays Biochem 47, 53–67. [PubMed: 20533900]

Khan GA, Girish GV, Lala N, Di Guglielmo GM and Lala PK 2011 Decorin is a novel VEGFR-2-binding antagonist for the human extravillous trophoblast. Mol Endocrinol 25, 1431–1443. [PubMed: 21659473]

Kilburn BA, Wang J, Duniec-Dmuchowski ZM, Leach RE, Romero R. and Armant DR 2000 Extracellular matrix composition and hypoxia regulate the expression of HLA-G and integrins in a human trophoblast cell line. Biology of reproduction 62, 739–747. [PubMed: 10684818]

Lagakos S, Wessen B. and Zelen M. 1986 An analysis of contaminated well water and health eff ects in Woburn, Massachusetts Journal of the American Statistical Association 81, 583–596.

Laham S. 1970 Studies on placental transfer. Trichlorethylene. IMS Ind Med Surg 39, 46–49. [PubMed: 5263053]

Author Manuscript Author Manuscript Author Manuscript Author Manuscript

Lash LH and Anders MW 1986 Cytotoxicity of S-(1,2-dichlorovinyl)glutathione and S-(1,2-dichlorovinyl)-L-cysteine in isolated rat kidney cells. J Biol Chem 261, 13076–13081.

Lash LH and Anders MW 1987 Mechanism of S-(1,2-dichlorovinyl)-L-cysteine-and S-(1,2-dichlorovinyl)-L-homocysteine-induced renal mitochondrial toxicity. Molecular pharmacology 32, 549–556. [PubMed: 3670284]

Lash LH, Chiu WA, Guyton KZ. and Rusyn I. 2014 Trichloroethylene biotransformation and its role in mutagenicity, carcinogenicity and target organ toxicity. Mutat Res Rev Mutat Res 762, 22–36. [PubMed: 25484616]

Lash LH, Fisher JW, Lipscomb JC and Parker JC 2000a Metabolism of trichloroethylene. Environ Health Perspect 108 Suppl 2, 177–200.

Lash LH, Hueni SE and Putt DA 2001 Apoptosis, necrosis, and cell proliferation induced by S-(1,2-dichlorovinyl)-L-cysteine in primary cultures of human proximal tubular cells. Toxicol Appl Pharmacol 177, 1–16. [PubMed: 11708895]

Lash LH, Parker JC and Scott CS 2000b Modes of action of trichloroethylene for kidney tumorigenesis. Environ Health Perspect 108 Suppl 2, 225–240.

Lash LH, Putt DA, Brashear WT, Abbas R, Parker JC and Fisher JW 1999 Identification of S-(1,2-dichlorovinyl)glutathione in the blood of human volunteers exposed to trichloroethylene. J Toxicol Environ Health A 56, 1–21. [PubMed: 9923751]

Lash LH, Putt DA, Hueni SE, Krause RJ and Elfarra AA 2003 Roles of necrosis, Apoptosis, and mitochondrial dysfunction in S-(1,2-dichlorovinyl)-L-cysteine sulfoxide-induced cytotoxicity in primary cultures of human renal proximal tubular cells. J Pharmacol Exp Ther 305, 1163–1172. [PubMed: 12626654]

Lattuada D, Colleoni F, Martinelli A, Garretto A, Magni R, Radaelli T. and Cetin I. 2008 Higher mitochondrial DNA content in human IUGR placenta. Placenta 29, 1029–1033. [PubMed: 19007984]

Lee HJ, Jeong SK, Na K, Lee MJ, Lee SH, Lim JS, Cha HJ., Cho JY, Kwon JY, Kim H, Song SY, Yoo JS, Park YM, Kim H, Hancock WS and Paik YK 2013 Comprehensive genome-wide proteomic analysis of human placental tissue for the Chromosome-Centric Human Proteome Project. J Proteome Res 12, 2458–2466. [PubMed: 23362793]

Loch-Caruso R, Hassan I, Harris SM, Kumar A, Bjork F. and Lash LH 2018 Trichloroethylene exposure in mid-pregnancy decreased fetal weight and increased placental markers of oxidative stress in rats. Reprod Toxicol 83, 38–45. [PubMed: 30468822]

Mando C, De Palma C, Stampalija T, Anelli GM, Figus M, Novielli C, Parisi F, Clementi E, Ferrazzi E. and Cetin I. 2014 Placental mitochondrial content and function in intrauterine growth restriction and preeclampsia. American journal of physiology. Endocrinology and metabolism 306, E404–413. [PubMed: 24347055]

McKinney LL, Picken JC Jr., Weakley FB, Eldridge AC, Campbell RE, Cowan JC and Biester HE 1959 Possible Toxic Factor of Trichloroethylene-extracted Soybean Oil Meal3. Journal of the American Chemical Society 81, 909–915.

Morgan T. 2014 Placental Insufficiency Is a Leading Cause of Preterm Labor. NewReviews 15, 5618-e5525.

Morgan TK 2016 Role of the Placenta in Preterm Birth: A Review. Am J Perinatol 33, 258–266. [PubMed: 26731184]

Myllynen P, Pasanen M. and Pelkonen O. 2005 Human placenta: a human organ for developmental toxicology research and biomonitoring. Placenta 26, 361–371. [PubMed: 15850640]

Nishimura M. and Naito S. 2006 Tissue-specific mRNA expression profiles of human phase I metabolizing enzymes except for cytochrome P450 and phase II metabolizing enzymes. Drug Metab Pharmacokinet 21, 357–374. [PubMed: 17072089]

NTP. 2015 National Toxicology Progam Monograph on Trichloroethylene Reports on Carcinogens, National Toxicology Progam.

OSHA. 2019 Occupational Safety and Health Administration Annotated OSHA Z-2 Table. Occupational Safety and Health Administration.

Author Manuscript Author Manuscript Author Manuscript Author Manuscript

Oshvandi K, Jadidi A, Dehvan F, Shobeiri F, Cheraghi F, Sangestani G, Moghadari Koosha B, Takarli F. and Aghababaie S. 2018 Relationship between Pregnancy-induced Hypertension with Neonatal and Maternal Complications. International Journal of Pediatrics 6, 8587–8594.

Pereira LC, Miranda LF, de Souza AO and Dorta DJ 2014 BDE-154 induces mitochondrial permeability transition and impairs mitochondrial bioenergetics. J Toxicol Environ Health A 77, 24–36. [PubMed: 24555644]

Poidatz D, Dos Santos E, Duval F, Moindjie H, Serazin V, Vialard F, De Mazancourt P. and Dieudonne MN 2015 Involvement of estrogen-related receptor-gamma and mitochondrial content in intrauterine growth restriction and preeclampsia. Fertil Steril 104, 483–490. [PubMed: 26051094]

Ruckart PZ, Bove FJ and Maslia M. 2014 Evaluation of contaminated drinking water and preterm birth, small for gestational age, and birth weight at Marine Corps Base Camp Lejeune, North Carolina: a cross-sectional study. Environ Health 13, 99. [PubMed: 25413571]

Rusyn I, Chiu WA, Lash LH, Kromhout H, Hansen J. and Guyton KZ 2014 Trichloroethylene: Mechanistic, epidemiologic and other supporting evidence of carcinogenic hazard. Pharmacol Ther 141, 55–68. [PubMed: 23973663]

Sanchez-Aranguren LC, Espinosa-Gonzalez CT, Gonzalez-Ortiz LM, Sanabria-Barrera SM, Riano-Medina CE, Nunez AF, Ahmed A, Vasquez-Vivar J. and Lopez M. 2018 Soluble Fms-Like Tyrosine Kinase-1 Alters Cellular Metabolism and Mitochondrial Bioenergetics in Preeclampsia. Front Physiol 9, 83. [PubMed: 29563877]

Stark G. 2005 Functional consequences of oxidative membrane damage. J Membr Biol 205, 1–16. [PubMed: 16245038]

Takao T, Asanoma K, Kato K, Fukushima K, Tsunematsu R, Hirakawa T, Matsumura S, Seki H, Takeda S. and Wake N. 2011 Isolation and characterization of human trophoblast side-population (SP) cells in primary villous cytotrophoblasts and HTR-8/SVneo cell line. PloS one 6, e21990.

Takara. 2013a Human Mitochondrial DNA (mtDNA) Monitoring Primer Set Cat. # 7246 Product Manual Takara Bio Inc, Mountain View, California.

Takara. 2013b UTF-8'en-us'mtDNA_Copy_Number_Calculation In: UTF-8'en-us'mtDNA_Copy_Number_Calculation (Ed), Microsoft Excel, Takara Bio Inc, Mountain View, California.

Tetz LM, Cheng AA, Korte CS, Giese RW, Wang P, Harris C, Meeker JD and Loch-Caruso R. 2013 Mono-2-ethylhexyl phthalate induces oxidative stress responses in human placental cells in vitro. Toxicol Appl Pharmacol 268, 47–54. [PubMed: 23360888]

Traber MG and Atkinson J. 2007 Vitamin E, antioxidant and nothing more. Free Radic Biol Med 43, 4–15. [PubMed: 17561088]

van de Water B, Zoeteweij JP, de Bont HJ, Mulder GJ and Nagelkerke JF 1994 Role of mitochondrial Ca2+ in the oxidative stress-induced dissipation of the mitochondrial membrane potential. Studies in isolated proximal tubular cells using the nephrotoxin 1,2-dichlorovinyl-L-cysteine. J Biol Chem 269, 14546–14552.

van de Water B, Zoeteweij JP, de Bont HJ and Nagelkerke JF 1995 Inhibition of succinate:ubiquinone reductase and decrease of ubiquinol in nephrotoxic cysteine S-conjugate-induced oxidative cell injury. Molecular pharmacology 48, 928–937. [PubMed: 7476924]

Vaughan OR and Fowden AL. 2016 Placental metabolism: substrate requirements and the response to stress. Reprod Domest Anim 51 Suppl 2, 25–35.

Walker DI., Uppal K, Zhang L, Vermeulen R, Smith M, Hu W, Purdue MP, Tang X, Reiss B, Kim S, Li L, Huang H, Pennell KD, Jones DP, Rothman N. and Lan Q. 2016 High-resolution metabolomics of occupational exposure to trichloroethylene. Int J Epidemiol 45, 1517–1527. [PubMed: 27707868]

Waters EM, Gerstner HB and Huff JE 1977 Trichloroethylene. I. An overview. J Toxicol Environ Health 2, 671–707. [PubMed: 403297]

Wu Z, Mao W, Yang Z, Lei D, Huang J, Fan C. and Suqing W. 2019 Knockdown of CYP1B1 suppresses the behavior of the extravillous trophoblast cell line HTR-8/SVneo under hyperglycemic condition. J Matern Fetal Neonatal Med, 1–12.

Author Manuscript Author Manuscript Author Manuscript Author Manuscript

Xu F, Papanayotou I, Putt DA, Wang J. and Lash LH 2008 Role of mitochondrial dysfunction in cellular responses to S-(1,2-dichlorovinyl)-L-cysteine in primary cultures of human proximal tubular cells. Biochem Pharmacol 76, 552–567. [PubMed: 18602084]

Zdravkovic M, Aboagye-Mathiesen G, Guimond MJ, Hager H, Ebbesen P. and Lala PK 1999 Susceptibility of MHC class I expressing extravillous trophoblast cell lines to killing by natural killer cells. Placenta 20, 431–440. [PubMed: 10419808]

Zorov DB, Filburn CR, Klotz LO, Zweier JL and Sollott SJ 2000 Reactive oxygen species (ROS)-induced ROS release: a new phenomenon accompanying induction of the mitochondrial permeability transition in cardiac myocytes. J Exp Med 192, 1001–1014. [PubMed: 11015441]

Zorov DB, Juhaszova M. and Sollott SJ. 2014 Mitochondrial reactive oxygen species (ROS) and ROS-induced ROS release. Physiol Rev 94, 909–950. [PubMed: 24987008]

Author Manuscript Author Manuscript Author Manuscript Author Manuscript

## Highlights

- DCVC decreased mitochondrial content in HTR-8/SVneo placental trophoblasts.
- DCVC induced adaptive and subsequently pathogenic mitochondrial perturbations.
- (±)-α-tocopherol attenuated DCVC-induced mitochondrial membrane depolarization.
- (±)-α-tocopherol failed to attenuate DCVC-induced oxygen consumption perturbations.
- Mitochondria are prominent intracellular targets of DCVC injury in placental cells.

Author Manuscript Author Manuscript Author Manuscript Author Manuscript

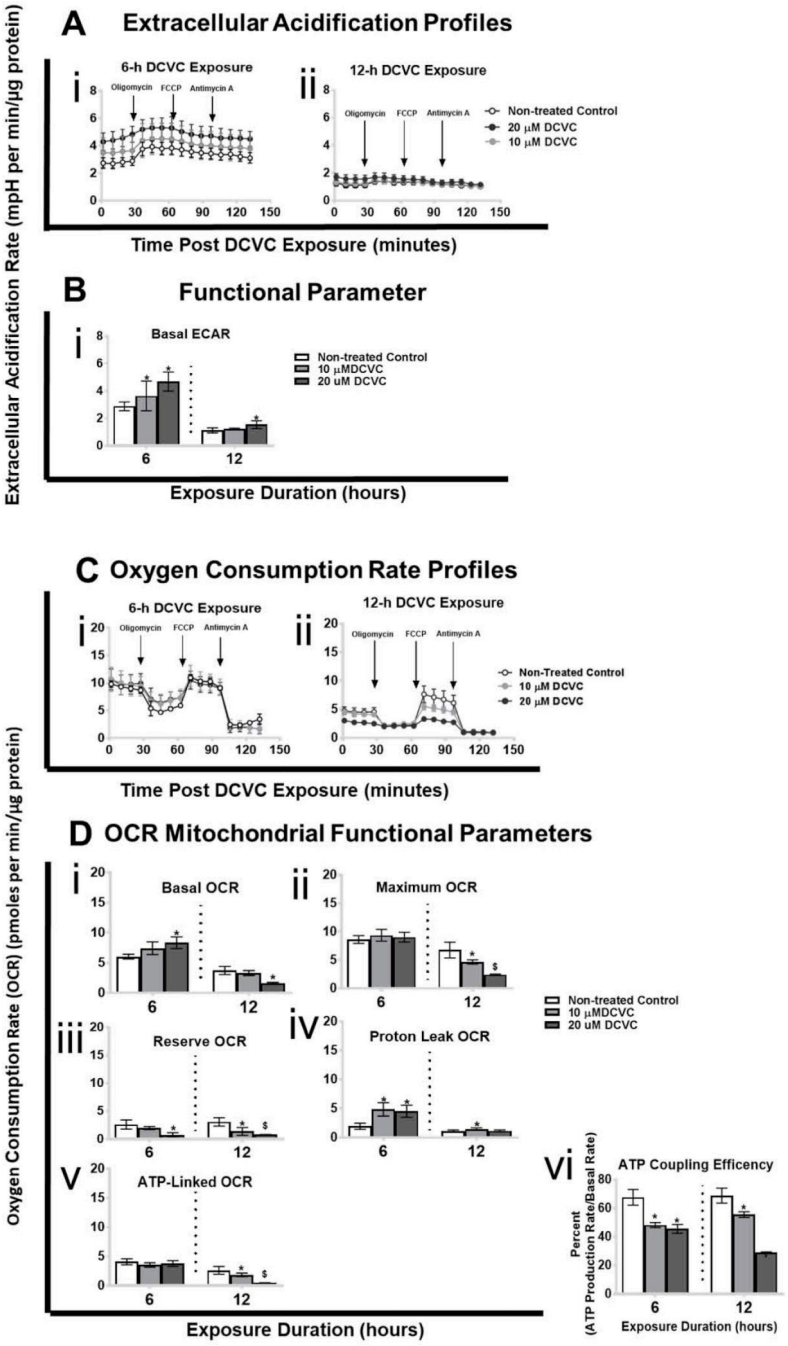


**Figure 1. Effects of DCVC on extracellular acidification rate (ECAR), oxygen consumption rate (OCR) and mitochondrial functional parameters.**

Cells were treated for 6 or 12 h with medium alone (control), or with 10 or 20 μM DCVC. Following exposure, ECAR and OCR were measured simultaneously in real-time using the Seahorse XF24e or XF24 analyzers. Key mitochondrial functional parameters were assessed by serially injecting compounds that target specific portions of the electron transport chain (oligomycin, FCCP, antimycin A/rotenone) into wells with the cells. Mitochondrial functional parameters were measured or calculated as described in the methods section. **A)**

Author Manuscript Author Manuscript Author Manuscript Author Manuscript

Extracellular acidification rate ECAR profiles following DCVC treatment for (**i**) 6 h and (**ii**) 12 h. Data points represent mean ECAR ± SEM at 5-minute intervals. **B)** ECAR functional parameter: basal ECAR. **C)** Oxygen consumption rate profiles following DCVC treatment for (**i**) 6 h and (**ii**) 12 h. Data are graphed as mean OCRs ± SEM at 5-minute intervals. Arrows indicate times when electron transport chain modifiers were injected into sample wells. **D)** OCR functional parameters: (**i**) basal OCR, (**ii**) maximum OCR, (**iii**) reserve OCR, (**iv**) proton leak OCR, (**v**) ATP-linked OCR, and (**vi**) ATP coupling efficiency. Bars represent means ± SEM. Data were analyzed by adjusted linear mixed-models with posthoc Tukey multiple comparisons restricted to comparison within each time point because experiments were conducted separately (as indicated by vertical dashed line on graph). Asterisk indicates significant difference compared to controls within same time point: *$P<0.05$. Dollar sign indicates significant difference compared to controls and 10 μM DCVC within same time point: $^{\$}P<0.05$. N= 3 independent experiments for each time point.

Author Manuscript Author Manuscript Author Manuscript Author Manuscript

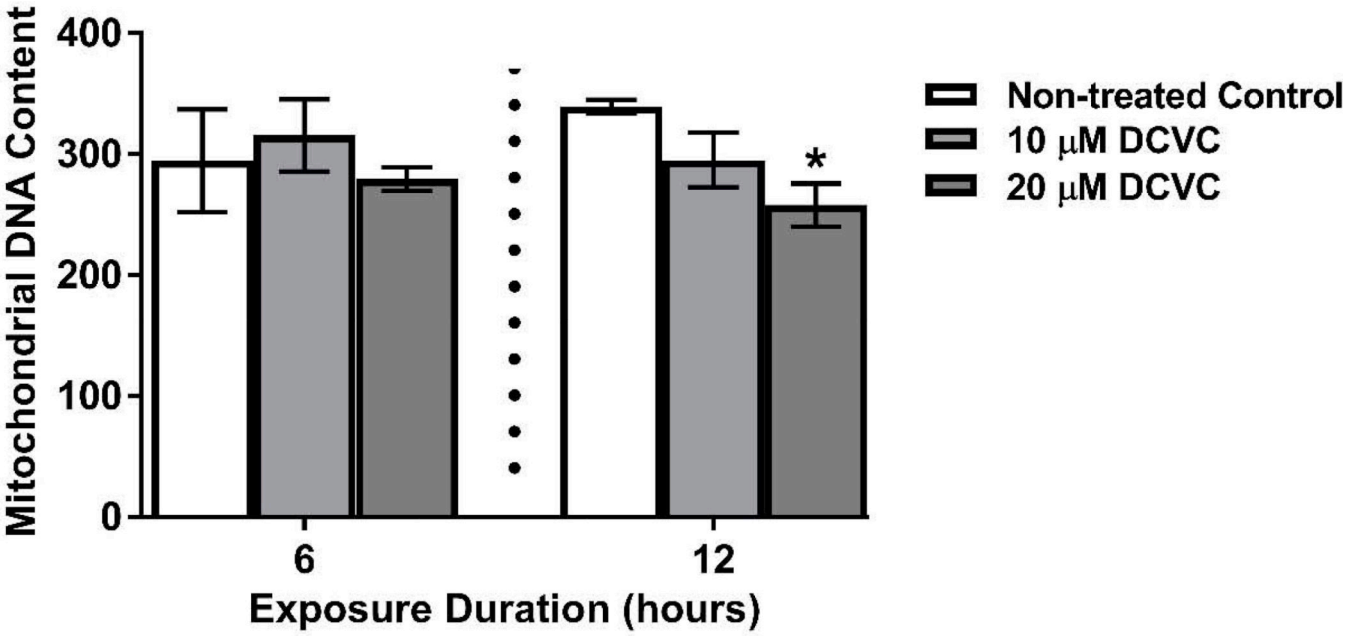


**Figure 2. Effects of DCVC mitochondrial DNA content.**

Cells were treated for 6 or 12 h with medium alone (control), or with 10 or 20 μM DCVC. Mitochondrial DNA content, a proxy for mitochondrial copy number, was estimated by measuring genomic DNA of two mitochondrial genes and two nuclear genes, and calculating the ratios: *ND1/SLCO2B1* and *ND5/SERPINA1*. Bars represent means ± SEM. Data were analyzed by one-way ANOVA with posthoc Tukey's multiple comparisons within each time point because experiments were conducted separately (as indicated by vertical dashed line on graph). Asterisk indicates significant difference compared to control within the same time point: *P =0.0192. N=3 independent experiments for the 6-h time point and N=4 independent experiments for the 12-h time point.

Author Manuscript Author Manuscript Author Manuscript Author Manuscript

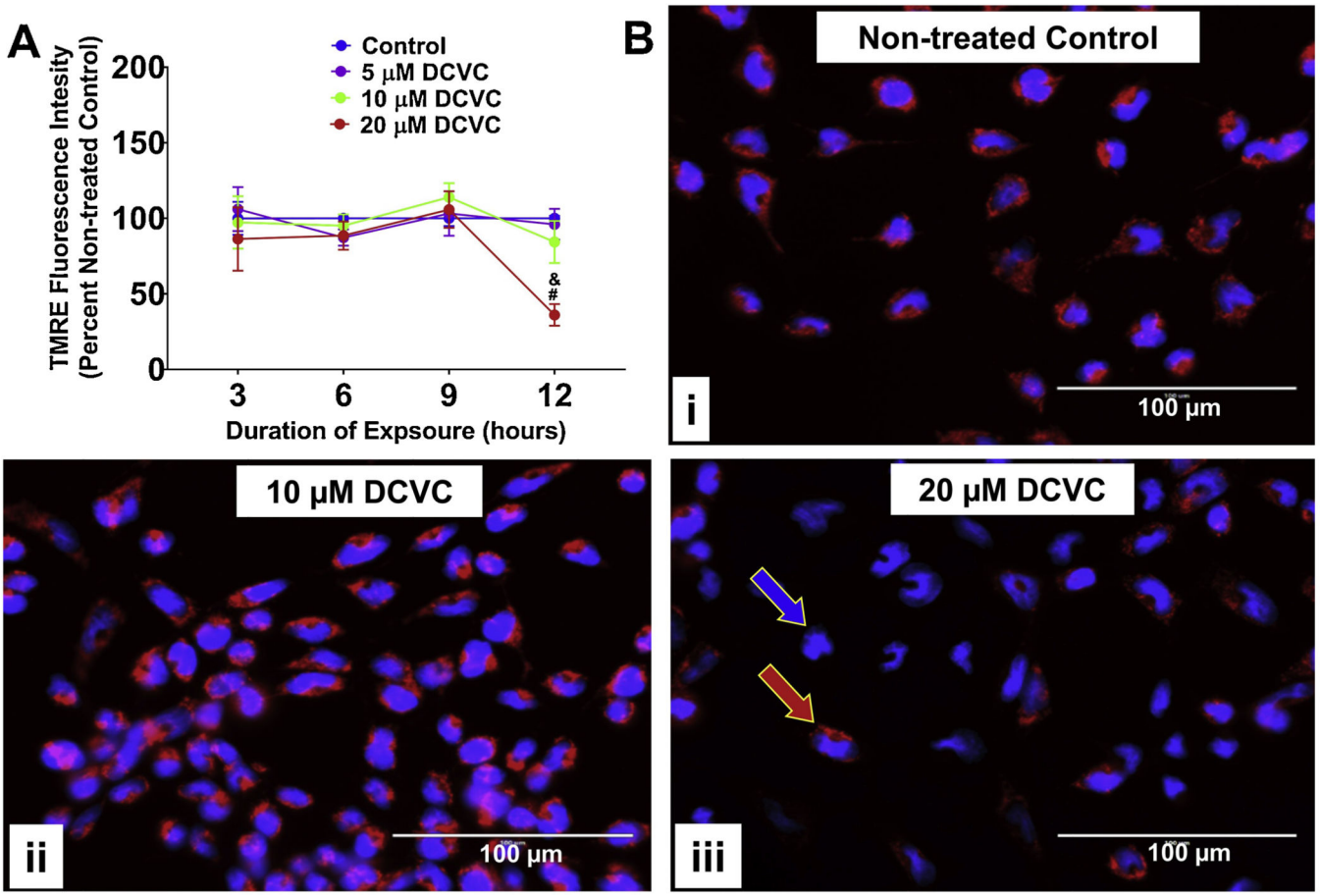


**Figure 3. Effects of DCVC mitochondrial membrane potential.**

**A)** Graphical representation of mitochondrial membrane potential expressed as percent non-treated control. Cells were treated for 3, 6, 9 or 12 h with medium alone (control), or with 5, 10, or 20 µM DCVC. Tetramethylrhodamine ethyl ester (TMRE), a cell-permanent fluorochrome, was used to measure relative mitochondrial membrane potential. The fluorescence signal is proportional to mitochondrial membrane polarization. N= 3 independent experiments for each time point, with 4 replicates per treatment in each experiment. Data are graphed as means ± SEM. Data were analyzed by two-way ANOVA (no significant interaction detected between time and treatment, P=0.1533) with posthoc Tukey multiple comparisons. Ampersand sign indicates significant difference compared to control, 5 µM DCVC and 10 µM DCVC within the same time point: $^{\&}P = 0.0013$. Pound sign indicates significant difference compared to same treatment at all earlier time points: $^{\#}P < 0.001$. FCCP (10 µM) was included as a positive control and depolarized the mitochondrial membrane potential by 16.45% ± 4.19% at 3 h, 18.9% ± 4.16% at 6 h, 24.13% ± 7.89% at 9 h, and 8.78% ± 8.78% at 12 h. **B)** Visualization of DCVC-induced depolarization of mitochondrial membrane potential by fluorescence microscopy. Cells were treated for 12 hours with (**i**) 0 µM DCVC (control), (**ii**) 10 µM DCVC or (**iii**) 20 µM DCVC. Red fluorescence (TMRE) represents normal mitochondrial membrane potential (red arrow). Blue fluorescence (Hoechst stain) represents cellular nuclei (blue arrow). All images shown with 100 µm scale bars. Representative images from 3 experiments are shown.

Author Manuscript Author Manuscript Author Manuscript Author Manuscript

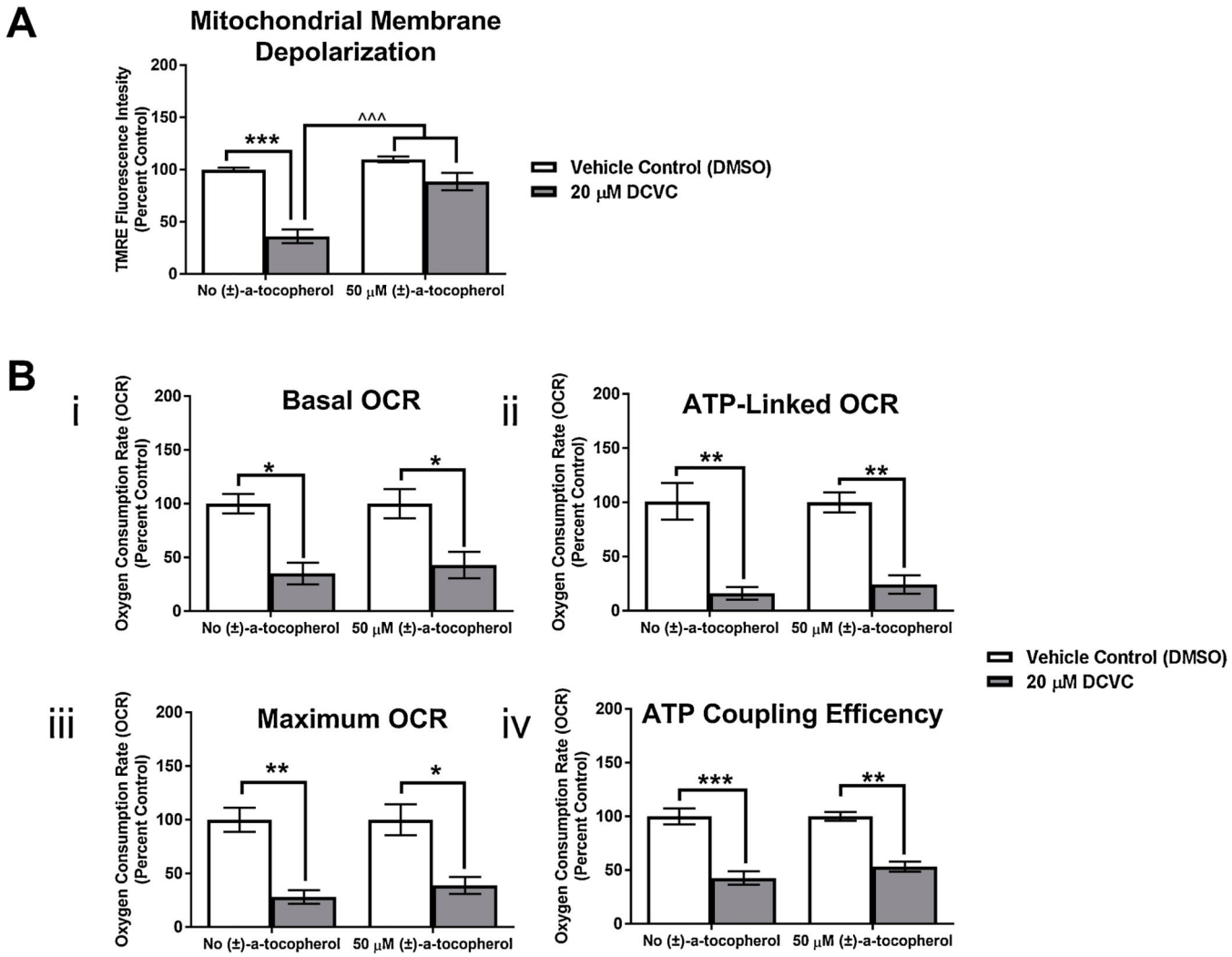


**Figure 4. Effect of antioxidant co-treatment on DCVC-induced changes in membrane potential depolarization and OCR.**

Cells were treated with DMSO (vehicle control for α-tocopherol) or 20 μM DCVC with or without 50 μM (±) α-tocopherol (pre-treatment for 15 min followed by co-treatment for 12 h). A) Modulation of DCVC-induced relative mitochondrial membrane potential depolarization as measured using TMRE fluorescence. B) Failed modulation of DCVC-induced OCR perturbations as measured by the Seahorse XF analyzer including: (**i**) basal OCR, (**ii**) ATP-linked OCR, (**iii**) maximum OCR, and (**iv**) ATP coupling efficiency. Bars represent means ± SEM as percent control. Data were analyzed by two-way ANOVA prior to percent control conversion (attenuation of membrane potential depolarization had interaction between DCVC and (±) α-tocopherol treatments, P= 0.0052; no other significant interaction detected), followed by Tukey's multiple comparison of means. Asterisk indicates significant differences compared to vehicle control with no (±) α-tocopherol treatment or vehicle control with (±) α-tocopherol treatment: *P≤0.016, **P ≤0.0043, ***P =0.005. Circumflex accent sign indicates significant difference compared to 20 μM DCVC with no (±) α-tocopherol treatment: ^^^P ≤ 0.0007. N= 3 independent experiments, with 4 replicates per treatment in each experiment.

Author Manuscript Author Manuscript Author Manuscript Author Manuscript

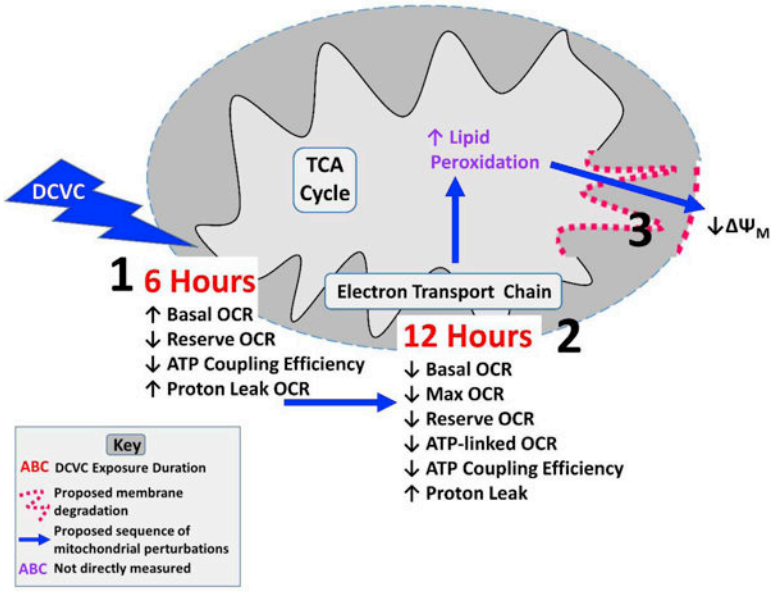


**Figure 5. Proposed DCVC-induced mitochondrial dysfunction in HTR-8/SVneo cells.**

Overview and proposed partial sequence of DCVC-induced perturbations impacting mitochondrial structure and function. 1) At 6 h, mitochondrial basal OCR, reserve OCR and proton leak rate were elevated, while ATP coupling efficiency dropped significantly. 2) At 12 h, basal OCR declined significantly, accompanied by diminished maximum and reserve OCR, reduced ATP-linked OCR and decreased coupling efficiency, suggesting time-dependent progressive mitochondrial dysfunction. 3) Between 9 and 12 h, lipid peroxidation contributed to depolarization of mitochondrial membrane potential, however it did not contribute to other oxygen consumption-related mitochondrial perturbations, indicating lipid peroxidation may be a secondary effect of mitochondrial dysfunction.